Effects of lateral diffusion on the fluorescence anisotropy in hexagonal lipid phases

II. An experimental study

Sun-Yung Chen,* Kwan Hon Cheng,* B. Wieb Van Der Meer,‡ and Joseph M. Beechem§

*Department of Physics, Texas Tech University, Lubbock, Texas 79409; ‡Department of Physics and Astronomy, Western Kentucky University, Bowling Green, Kentucky 42101; and §Department of Molecular Physiology and Biophysics, Vanderbilt University, Nashville, Tennessee 37232 USA

ABSTRACT The polymorphic phase behavior of unsaturated phosphatidylethanolamine (PE)/diacylglycerol (DG) binary lipid mixtures was investigated by the use of time-resolved fluorescence anisotropy. Using a fluorescent lipid, 1-palmitoyl-2-[[2-[4-(6-phenyl-trans-1,3,5-hexatrienyl)phenylethyl]carbonyl]3-*sn*-phosphatidyl-choline (DPH-PC), the orientational order and rotational dynamics of the above lipid mixtures in the liquid crystalline lamellar (L_α) and inverted hexagonal (H_{II}) phases were studied. By employing a one-exponential model (Cheng, K. H. 1989. *Biophys. J.* 55:1025–1031) to fit the anisotropy decay data, abrupt decreases in the normalized initial anisotropy decay slope and the residual anisotropy of DPH-PC were observed at ~6–8% DG, signifying a L_α/H_{II} phase transition. Using our new theoretical WOBHOP and P2P4HOP models as described in a preceding paper (Van Der Meer, B. W., K. H. Cheng, and S. Y. Chen. 1990. *Biophys. J.* 58:000–000), two or more rotational correlation times were required to describe the anisotropy decay behavior of DPH-PC in the H_{II} phase. These rotational correlation times were further related to the second and fourth rank order parameters, and the wobbling and hopping diffusion constants of the fluorescent probe in the highly curved lipid cylindrical tubes of the H_{II} phase. The hopping diffusion constant (D_H) equals the lateral diffusion constant (D_L) divided by R^2 (R = radius of the lipid cylindrical tubes). The value of D_L was estimated by measuring the excimer formation rate of 1-palmitoyl-2-[10-(1-pyrenl)decanoyl] phosphatidyl choline (py-PC) in the same PE/DG mixtures. Upon comparing the values of D_H and D_L, the value of R was determined to be ~10–15 Å, and agreed with that derived from x-ray diffraction (Tate, M. W., and S. M. Gruner. 1989. *Biochemistry.* 28:4245–4253; Rand, R. P., N. L. Fuller, S. M. Gruner, and V. A. Parsegian. 1990. *Biochemistry.* 29:76–87).

INTRODUCTION

Among various lipid phase transitions, the lamellar liquid crystalline (L_α) to inverted hexagonal (H_{II}) phase transition has gained a remarkable resurgence of interest in recent years (Cheng, 1989*a–c*; Tate and Gruner, 1989; van Langen et al., 1989). Although the fully hydrated L_α phase appears to be the most commonly known structural phase for both biological and synthetic lipids in aqueous dispersions, nonlamellar phases, e.g., H_{II} phase, can also occur for several lipid/water mixtures (Cheng, 1989*a–c*) and biological systems (Crowe and Crowe, 1982). The interest in studying the inverted hexagonal phase of lipids stems from the experimentally observed correlation between the lipid nonbilayer structures and the membrane-related functions, such as ion transport of membrane protein (Cheng et al., 1986*a* and *b*) and membrane fusion (Ellens et al., 1989).

The basic morphological structures of L_α and H_{II} phases have been studied for quite some time (Luzzati, 1962). In the L_α phase, the molecules are arranged in a one-dimensional lattice which consists of stacked lipid bilayers with layers of water between the polar surfaces of the lipids. However, in the H_{II} phase, the molecules rearrange themselves to form a two-dimensional hexagonal lattice in which the lipid molecules form long water-cored cylindrical tubes with the polar head groups facing inside. Therefore, the L_α to H_{II} phase transition involves changes not only in the lipid surface curvature but also in the packing geometry of the lipids. The latter involves a significant topological rearrangement of lipid and water molecules from a one-dimensional to a two-dimensional packing symmetry (Kirk and Gruner, 1985). To understand the mechanism underlying this phase transition, more detailed studies on the microscopic structures and molecular dynamics in both phases are required.

A study of the time-resolved fluorescence anisotropy decay of fluorescent probes embedded in lipid suspensions provides information regarding the orientational order and the rotational dynamics of the lipids (Szabo, 1980; Zannoni et al., 1983; Van Der Meer et al., 1984). This time-resolved fluorescence anisotropy decay method has been successfully applied to study the lipid dynamics of various lamellar phases (Ameloot et al., 1984; Van Der Meer et al., 1984). Yet its application to nonlamellar phases has just been initiated quite recently (Cheng, 1989*a–c*). In our preceding paper, new theoretical models for the anisotropy decay of fluorophore in the H_{II} phase were presented. To demonstrate the application of these

Address correspondence to Dr. Cheng.

0006-3495/90/12/1527/11 $2.00

new models, we chose a binary lipid mixture which exhibits L_α, H_{II}, and L_α/H_{II} coexisting phases.

The binary lipid mixture employed in this study consists of unsaturated phosphatidylethanolamine (PE) and diacylglycerol (DG). As a breakdown product of membrane phosphatidylinositol turnover, DG exhibits a strong structural perturbation effect on the lipid bilayer phase. This bilayer disruption characteristic of DG was shown to relate with the activation of membrane protein activity (Cheng et al., 1986*b*) and quite recently the promotion of membrane fusion (Siegel et al., 1989). An unsaturated DG, diolein, was used in this study. The phase behavior of this PE/DG binary mixture has been determined previously by x-ray diffraction, ^{31}P NMR and differential scanning calorimetry (Das and Rand, 1986; Epand et al., 1988; Siegel et al., 1989).

By applying our new theoretical WOBHOP and P2P4HOP models (see the preceding paper), the local second and fourth orientational order parameters ($\langle P_2 \rangle$ and $\langle P_4 \rangle$) and wobbling diffusion constant of a fluorescent lipid, 1-palmitoyl-2-[[2-[4-(6-phenyl-trans-1,3,5-hexatrienyl)phenyl]ethyl]carbonyl]3-*sn*-phosphatidylcholine (DPH-PC), with respect to the local symmetry axis of the lipids were determined in the L_α, H_{II}, and L_α/H_{II} coexisting phases. The advantages of using this fluorescent lipid probe DPH-PC over the other lipophilic probes in studying the L_α-H_{II} phase transition have been discussed elsewhere (Cheng, 1989*a*). From the theoretical models, an extra mode of diffusional motion (hopping motion), which refers to the rotational diffusion of the fluorophore with its axis of rotation along the long symmetry axis of the lipid tubes, was also determined. Theoretically, this hopping motion is related with the geometrical size of the hexagonally packed lipid tubes and the lateral diffusion constant of the lipids. To confirm the correlation between this hopping motion and the lateral diffusion of the lipids, pyrene excimer formation technique was employed to independently measure the lateral diffusion constant of the lipids. From these hopping and lateral diffusion constants, the radius of the lipid tubes was determined and compared with that derived from x-ray diffraction (Tate and Gruner, 1989; Rand et al., 1990).

MATERIALS AND METHODS

Sample preparation

PE transphosphatidylated from egg phosphatidylcholine(PC) (TPE) and 1,2-dioleoyl-*sn*-glycerol (diolein) were obtained from Avanti Polar Lipids (Birmingham, AL). 1-palmitoyl-2-[[2-[4-(6-phenyl-trans-1,3,5-hexatrienyl)phenyl]ethyl]carbonyl]-3-*sn*-PC (DPH-PC) and 1-palmitoyl-2-[10-(1-pyrenyl)decanoyl]-PC (py-PC) were obtained from Molecular Probes, Inc. (Eugene, OR). All lipids were dissolved in chloroform at −30°C and were used without further purification. The fluorescent probe and lipid were first mixed in chloroform (spectroscopic grade). The molar ratio of DPH-PC to total lipid was 0.2% for the fluorescence lifetime and emission anisotropy decay measurements. In pyrene excimer formation measurements, the molar ratio of py-PC to total lipid (Xpyr) was maintained at 2%. The mixture was dried under a gentle nitrogen stream in a clean pyrex tube and further kept in vacuum for at least 4 h to ensure complete removal of the residual chloroform. The thin film formed on the tube was then hydrated with an aqueous buffer (100 mM NaCl, 10 mM TES, and 2 mM EDTA pH = 7.4) at 4°C. The suspension thus formed was vortexed rigorously and placed under mild sonication in a bath sonicator for a few seconds. The resulting suspension was then incubated overnight at 4°C in the dark to ensure proper hydration. Upon further dilution to ~0.15 mg/ml, the sample was then placed in a 10-mm UV quartz cuvette for subsequent fluorescence measurements. To eliminate oxygen quenching in pyrene excimer formation measurements, the buffer was purged with dry nitrogen gas before use. Also, the sample chamber of the fluorometer was purged with dry nitrogen during the fluorescence measurements.

Instrumentation

Fluorescence measurements were performed on a frequency domain cross-correlation fluorometer (ISS Inc., Champaign, IL). The excitation source was a Liconix 4240NB cw He-Cd laser (Santa Clara, CA) with an output of 17 mW at 325 nm. The operational principle of this continuously variable frequency phase-modulation fluorometer has been described elsewhere (Gratton et al., 1984; Lakowicz and Maliwal, 1985).

Fluorescence intensity decay measurements

Because the light exiting from the pockel cell (electro-optical device) is vertically polarized, a UV polarizer with the polarization axis set at 35° with respect to the vertical was placed in the excitation beam to eliminate the effect from rotational diffusion (Spencer and Weber, 1970). The fluorescence lifetime of DPH-PC was measured by using a nonfluorescent glycogen solution as a reference sample. A lower wavelength cutoff filter (model 3-72; Corning Glass-Works, Corning, NY) was used to remove the excitation light from the fluorescent signal and no filter was used for the reference sample. The phase delay ($\delta_F - \delta_S$) and modulation ratio (M_F/M_S) were measured at different modulation frequencies ranging from 1 to 230 MHz. Here δ_F and δ_S represent the phase delay of the signal by the fluorescent sample and that by the reference sample, respectively, and M_F and M_S represent the intensity modulation values of the fluorescent sample and that of the reference. The fluorescence lifetime of the py-PC monomer was measured at 380 nm through a monochromator (slit width = 2.0 nm). Both the phase delay and the modulation ratio of the py-PC fluorescence signal were compared with that of a standard solution (1,4-bis[2-(5-Phenyloxazolyl)]-benzene [POPOP] in methanol, lifetime = 1.419 ns) at different modulation frequencies ranging from 0.1 to 10 MHz.

Fluorescence anisotropy emission decay measurement

For time-resolved fluorescence anisotropy decay measurements, both excitation and emission polarizers were used (same emission filter). The differential polarized phase angle ($\delta_\perp - \delta_\parallel$) and the ratio of polarized modulation amplitudes ($M_\parallel/M_\perp$) were measured at different modulation frequencies (1–230 MHz). The subscripts $_\parallel$ and $_\perp$ refer to the directions of the polarization axis of the emission polarizer that are parallel and

perpendicular to the vertical axis, respectively. These values were measured using the L-format method (Lakowicz, 1983). The polarization axis of the excitation polarizer in our system was always set in the vertical direction.

Data analysis

a. Fluorescence emission anisotropy decay models

Various multi-exponential decay functions were employed to fit the fluorescence anisotropy decay data of DPH-PC. They all have the general form of

$$r(t) = r_\infty + (r_0 - r_\infty)\Sigma g_i e^{-A_i t}, \quad (1)$$

where r_0 and r_∞ are the initial and long time residuals of the anisotropy decay function. Here g_i and A_i are parameters defined below, and $\Sigma g_i = 1$.

1. One-exponential model:

$$r(t) = (r_0 - r_\infty) \exp(-t/\tau_1) + r_\infty \quad (2)$$

2. Two-exponential model:

$$r(t) = f_1 \exp(-t/\tau_1) + f_2 \exp(-t/\tau_2) + r_\infty \quad (3)$$

For the above two empirical models, τ_1 and τ_2 represent the rotational correlation times of the diffusional motion of the fluorophore, and f_1 and f_2 are their corresponding pre-exponential factors. Note that these two models do not provide detailed molecular information and parameters on the orientational packing and dynamics of the lipids.

3. WOBHOP model (see Eq. 9 in the preceding paper):

$$\begin{aligned} r(t) = {} & (r_0/4)(1 - \langle P_2\rangle^2) \exp(-t/\tau_W) \\ & + (3r_0/4)\langle P_2\rangle^2 \exp(-t/\tau_H) \\ & + (3r_0/4)(1 - \langle P_2\rangle^2) \exp[-t(1/\tau_W + 1/\tau_H)] \\ & + (r_0/4)\langle P_2\rangle^2, \end{aligned} \quad (4)$$

where $\langle P_2\rangle$ is the second rank order parameter, and τ_W and τ_H represent the correlation times of the fluorophore due to wobbling and hopping motions and are equal $(1 - \langle P_2\rangle^2)/(6D_W)$ and $1/(4D_H)$, respectively. Here D_W and D_H are the wobbling and hopping diffusion constants of the fluorophore.

If the correlation time of the hopping motion (τ_H) is much longer than that of the wobbling motion (τ_W), the anisotropy decay function described in the above WOBHOP model can be simplified into an equation containing two exponential decay terms. This simplified WOBHOP model is called reduced WOBHOP model and is shown below.

4. Reduced WOBHOP model:

$$\begin{aligned} r(t) = r_0[\langle P_2\rangle^2/4 + (1 - \langle P_2\rangle^2) \exp(-t/\tau_W) \\ + (3/4)\langle P_2\rangle^2 \exp(-t/\tau_H)]. \end{aligned} \quad (5)$$

The above Eq. 5 is then compared with the two-exponential model (Eq. 3). The fitting parameters of the two-exponential model can be expressed in terms of those of the WOBHOP model as follows:

$$\tau_1 = \tau_W \quad (6)$$

$$\tau_2 = \tau_H \quad (7)$$

$$r_\infty = r_0\langle P_2\rangle^2/4 \quad (8)$$

$$f_1 = r_0(1 - \langle P_2\rangle^2). \quad (9)$$

From the above equations, D_W, D_H, and $\langle P_2\rangle$ can be calculated directly from the fitting parameters of the two-exponential model and are shown below.

$$D_W = f_1/(6r_0\tau_1) \quad (10)$$

$$D_H = 1/(4\tau_2) \quad (11)$$

$$\langle P_2\rangle = [4r_\infty/(f_1 + 4r_\infty)]^{1/2}. \quad (12)$$

5. P2P4HOP model (see Eq. 12 in the preceding paper):

$$\begin{aligned} r(t) = {} & (r_0/4)[\langle P_2\rangle^2 + B_0 \exp(-C_0 t)][1 + 3 \exp(-t/\tau_H)] \\ & + B_1 \exp(-C_1 t)[\exp(-t/4\tau_H) + \exp(-t/\tau_H)] \\ & + (B_2/4) \exp(-C_2 t) \\ & \cdot [3 + 4 \exp(-t/4\tau_H) + \exp(-t/\tau_H)], \end{aligned} \quad (13)$$

where $\langle P_4\rangle$ is the fourth rank orientational order parameter. The pre-exponential factors B_i ($i = 0, 1, 2$) are functions of $\langle P_2\rangle$ and $\langle P_4\rangle$, while the exponential time constants C_i ($i = 0, 1, 2$) are functions of $\langle P_2\rangle$, $\langle P_4\rangle$, τ_W, and τ_H. They are shown in the Table 1.

In contrast to the one- and two-exponential model mentioned above, the WOBHOP, reduced WOBHOP and P2P4HOP models contain molecular parameters of the system. We therefore call them molecular models.

b. Data minimization

Single experiment anisotropy analyses were performed using ISS® routines (Urbana-Champaign, IL). The global anisotropy analyses were performed utilizing the Globals Unlimited® package (University of Illinois at Urbana-Champaign, IL). Rigorous confidence intervals were determined as described by Beechem and Haas (p 1230 of Beechem and Haas, 1989). Total intensity frequency domain data were analyzed utilizing the Marquardt algorithm (Gratton et al., 1984). The fluorescence intensity decay profiles of DPH-PC and py-PC monomer in PE/DG binary mixtures were fitted by a double-exponential function.

c. Lateral diffusion constant calculation

The monomer decay of py-PC was fitted by a double exponential decay function. A fixed short lifetime (5 ps) was used to fit the frequency domain data to take into account of the scattering contribution (Chong

TABLE 1 Pre-exponential factors and time constants in the P_2P_4HOP model (Eq. 13)

i	B_i	C_i
0	$1/5 + 2\langle P_2\rangle/7 + 18\langle P_4\rangle/35 - \langle P_2\rangle^2$	$(1 - \langle P_2\rangle^2)(1/5 + \langle P_2\rangle/7 - 12\langle P_4\rangle/35)/B_0\tau_W$
1	$1/5 + \langle P_2\rangle/7 - 12\langle P_4\rangle/35$	$(1 - \langle P_2\rangle^2)(1/5 + \langle P_2\rangle/14 - 8\langle P_4\rangle/35)/B_1\tau_W$
2	$1/5 - 2\langle P_2\rangle/7 + 3\langle P_4\rangle/35$	$(1 - \langle P_2\rangle^2)(1/5 - \langle P_2\rangle/7 - 2\langle P_4\rangle/35)/B_2\tau_W$

and Thompson, 1985). The monomer lifetime τ of py-PC is related to its excimer formation rate K_{dm} by the following relation

$$\tau^{-1} = K_r + K_{nr} + K_{dm} = \tau_0^{-1} + K_{dm}, \quad (14)$$

where K_r and K_{nr} are the radiative and nonradiative decay rates of pyrene molecule, respectively. τ_0 is the native lifetime of pyrene monomer in the absence of excimer formation. It has been shown that τ_0 of py-PC in lipids at 23°C is ~167 ns (Chong and Thompson, 1985). Note that Eq. 14 is valid under a reasonable assumption that the excimer dissociation rate is much smaller than K_{dm}. The lateral diffusion constant D_L is obtained from the following equation.

$$D_L = \langle n_s \rangle l^2 K_{dm}/4, \quad (15)$$

where l is the diffusion length and $\langle n_s \rangle$ is the average step number between two collision processes and is given by a random walk model (Galla et al., 1979),

$$\langle n_s \rangle = [2/\pi][1/X_{pyr}] \ln [2/X_{pyr}]. \quad (16)$$

RESULTS

Fluorescence lifetime

The fluorescence intensity decay measurements of DPH-PC in PE/DG mixtures of different compositions (0-18% DG) were performed at 13 different modulation frequencies (1, 2, 6, 10, 20, 30, 40, 60, 80, 100, 130, 150, and 170 MHz) and at 23°C. Using a two-exponential decay function to fit the frequency domain data, the values of lifetimes were found to be 6.5 and 0.05 ns. The molar fraction of the shorter lifetime was <4%. The origin of this extra lifetime of DPH-PC is attributed to the minor degraded product of the probe (Parente and Lentz, 1985; Cheng, 1989*a*, *b*). The values of the two lifetime components and their intensity fractions were found to be independent of DG composition (results not shown).

Fluorescence emission anisotropy decay

The fluorescence anisotropy decay measurements of DPH-PC in the same PE/DG mixtures were performed at 16 different modulation frequencies (1, 2, 10, 20, 30, 40, 50, 70, 90, 110, 130, 150, 170, 190, 210, and 230 MHz) and at 23°C. Fig. 1 *A* showed the typical values of the polarized modulation ratio and the differential polarized phase angle of the polarized fluorescence emission of DPH-PC in 18% DG lipid mixture as a function of modulation frequency.

One- and two-exponential models

As an initial step toward understanding the molecular dynamics behavior of DPH-PC in the PE/DG lipid system, both one- and two-exponential models were employed to fit the frequency domain data. From Eqs. 2 and 3, the fitting parameters involved were [f_1, τ_1, and r_∞] and [f_1, τ_1, f_2, τ_2, and r_∞] for the one- and two-exponential models, respectively. The fitted parameters and the chi-squares of different fits for DPH-PC in 0% and 18% DG mixtures were shown in Table 2, and the fitted curves for 18% DG were shown in Fig. 1 *A*. For 18% DG, the reduced chisquares of the fits were 1.82 and 0.96 for the one- and two-exponential models, respectively. The differences between the experimental and fitted values, i.e., residues, for both the phase and modulation data were plotted as a function of modulation frequency and shown in Figs. 1 *B* and *C*, respectively. It was evidenced from the plots that the residues of the two-exponential fit were more randomly distributed and smaller than that of the one-exponential fit. Similar observations were found for other samples with DG contents ranging from 10 to 18%. However, for the samples with DG contents ranging from 0 to 8%, the two-exponential model failed to provide a good fit to the frequency domain data when compared with the one-exponential model. Large uncertainties in the short rotational correlation time components were found. For example, a component of 0.186 ± 1.083 ns was obtained for DPH-PC in 0% DG using the two-exponential model as shown in Table 2.

The two parameters, r_∞/r_0 and $\dot{r}(0)/r_0$, represent the normalized long time residual and initial slope of the anisotropy decay of fluorophore in the lipid mixture. These two parameters were calculated from the fitted parameters of the decay functions, i.e., r_0 equals [$f_1 + r_\infty$] and [$f_1 + f_2 + r_\infty$] for the one- and two-exponential models, respectively. While $\dot{r}(0)/r_0$ equals $-[f_1/\tau_1]/r_0$ and $-[f_1/\tau_1 + f_2/\tau_2]/r_0$ for the one- and two-exponential models, respectively. The values of r_∞/r_0 were plotted as a function of DG% and shown in Fig. 2 *A*. The values of r_∞/r_0 obtained from the one-exponential model were always higher than that from the two-exponential model. Yet they all exhibited an abrupt decline at ~6–8% DG as the DG content increased from 0 to 18%. However, the r_∞/r_0 from the two-exponential model showed a more prominent drop (~40%) when compared with that from the one-exponential model (~16%). The values of $\dot{r}(0)/r_0$ were plotted as a function of DG% and shown in Fig. 2 *B*. For the one-exponential model, the values of $\dot{r}(0)/r_0$ were $\sim 20 \times 10^7\ s^{-1}$ for DG contents between 0 and 6%. As the DG content increased further, an abrupt decline occurred at ~6–8% DG. Thereafter, the $\dot{r}(0)/r_0$ remained relatively constant at $\sim 16 \times 10^7\ s^{-1}$ for DG contents between 10 and 18%. For the two-exponential model, the values of $\dot{r}(0)/r_0$ were not calculated for samples with low DG content (0–8%) due to the large uncertainties in the short correlation time components as mentioned above. For higher DG contents (10–18%), the $\dot{r}(0)/r_0$ was found to increase from $\sim 25 \times 10^7\ s^{-1}$ to $\sim 30 \times 10^7\ s^{-1}$ as the DG content increased from 10 to 18%. These values were

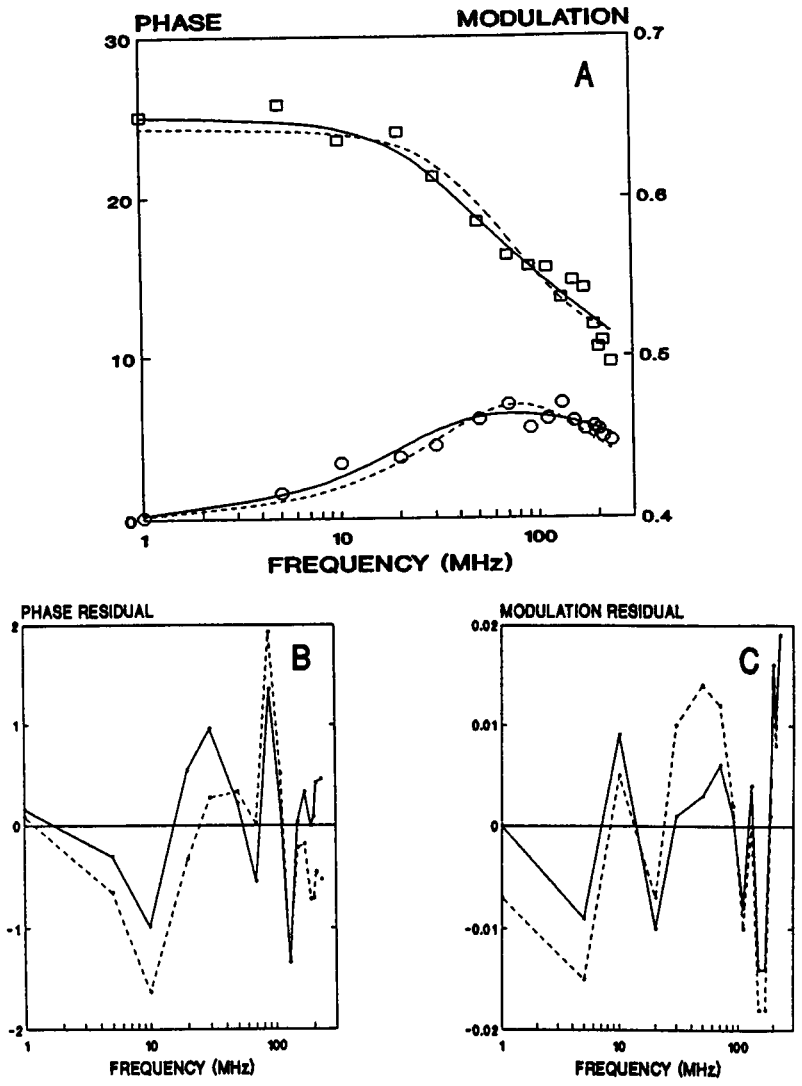

FIGURE 1 (*A*) Differential polarized phase angle (O) and ratio of polarized modulation (□) as a function of modulation frequency for DPH-PC in 18% DG mixture at 23°C. The solid and dotted line were obtained from the one- and two-exponential fits, respectively. The fitted parameters are shown in Table 2. (*B*) Residuals of the differential polarized phase angle from one-exponential fit (*dotted line*) and two-exponential fit (*solid line*) for DPH-PC in 18% DG. (*C*) Residuals of the ratio of polarized modulation from one-exponential fit (*dotted line*) and two-exponential fit (*solid line*) for DPH-PC in 18% DG.

higher than those obtained from the one-exponential model.

WOBHOP, reduced WOBHOP, and P2P4HOP models

Besides the empirical one and two-exponential models, a molecular model, namely, WOBHOP, was also employed to fit the data. This model involves a residual anisotropy and three exponential decay terms, yet there are only four parameters in the fitting. The parameters are D_W, D_H, $\langle P_2 \rangle$, and r_0. Fig. 3 showed the values of the parameters for DG varying from 0 to 18%. The values of $\langle P_2 \rangle$ were found to increase slightly with DG%. A significant decline in the values of D_W occurred for the DG content between 6 and 10%. The drop was >50%. The values of D_H were observed to increase from $\sim 5 \times 10^6\ s^{-1}$ to $\sim 3 \times 10^7\ s^{-1}$ as the DG content varied from 0 to 18%. Interestingly, the values of D_W were always larger than those of D_H for all DG%. During the fitting, the r_0 value was globally linked throughout all concentrations of DG (recovered value = 0.26).

As mentioned in Materials and Methods, the two-exponential model may also be used to calculate the physical parameters under the condition that the correla-

TABLE 2 Comparison the fitted and calculated parameters for one- and two-exponential models of the anisotropy decay profiles of DPH-PC in PE/DG mixtures

		Fitted parameters				
Sample	r_0	f_1	τ_1	f_2	τ_2	r_∞
			ns		*ns*	
1-exp 0% DG	0.22	0.094 ± 0.003	2.169 ± 0.245	—	—	0.130 ± 0.003
model 18% DG	0.25	0.136 ± 0.007	3.040 ± 0.293	—	—	0.112 ± 0.007
2-exp 0% DG	0.26	0.051 ± 0.278	0.186 ± 1.083	0.079	2.879 ± 0.449	0.130 ± 0.003
model 18% DG	0.26	0.060 ± 0.006	1.002 ± 0.194	0.104	10.02 ± 2.205	0.112 ± 0.007

		Calculated parameters				
Sample	r_∞/r_0	$\dot{r}(0)/r_0$	$\langle P_2 \rangle$	D_W	D_H	x^2
1-exp 0% DG	0.59	$19.7\times10^7 s^{-1}$	0.76	$3.22\times10^7 s^{-1}$	—	6.6
model 18% DG	0.45	$18.2\times10^7 s^{-1}$	0.67	$3.04\times10^7 s^{-1}$	—	1.7
2-exp 0% DG	0.50	$116.0\times10^7 s^{-1}$	0.95	$17.6\times10^7 s^{-1}$	$8.7\times10^7 s^{-1}$	7.3
model 18% DG	0.23	$28.4\times10^7 s^{-1}$	0.89	$3.8\times10^7 s^{-1}$	$2.5\times10^7 s^{-1}$	0.96

tion time of the hopping motion (τ_H) is much longer than that of the wobbling motion (τ_W). Using the results of the WOBHOP fitting, the values of τ_W and τ_H for the samples with DG contents >10% were ~0.8 and 12 ns, respectively. In other words, τ_H is about an order of magnitude longer than τ_W. Using Eqs. 10–12, the values of D_W, D_H, and $\langle P_2 \rangle$ were calculated and shown in Fig. 3. The values of the physical parameters obtained from this reduced WOBHOP model were found to be rather similar to that from the complete WOBHOP model.

A more intensive data fit using the P2P4HOP (Eq. 16) model was performed at 0 and 18% DG. The five physical parameters, D_W, D_H, $\langle P_2 \rangle$, $\langle P_4 \rangle$, and r_0, recovered from the P2P4HOP model are also shown in Table 3. The values of r_0 for both 0% and 18% DG were linked. The shapes of the residual plots of the linked fit of the P2P4HOP model were more randomly distributed than those of the WOBHOP model (see Figs. 4, *A* and *B*). The free two-exponential model for 18% DG also yielded adequate fits (see Table 2). For 0% DG, the hopping diffusion constant D_H obtained from either the WOBHOP or P2P4HOP model was quite small as compared with the wobbling diffusion constant D_W. On the contrary D_H was comparable to D_W for 18% DG. It was further noticed that the value of $\langle P_2 \rangle$ for 18% DG was significantly higher than that for 0% DG. Both the WOBHOP and the P2P4HOP models demonstrated that the value of $\langle P_2 \rangle$ for 18% DG is ~20% higher than that for 0% DG. Rigorous error analysis was performed for the data of 0 and 18% DG using the P2P4HOP model. In Table 3 lower and upper bounds of the 67% confidence intervals are reported for the parameters as well as their recovered values. Fig. 4 *C* shows a plot of the value of the lowest possible chisquare of the P2P4HOP model for 0% DG as a function of the value of D_H. This figure demonstrates that the hopping diffusion constant for 0% DG was statistically indistinguishable from zero. One distinctive feature of the P2P4HOP model is the estimation of the fourth rank order parameter $\langle P_4 \rangle$. From Table 3, the $\langle P_4 \rangle$ for 18% DG was found to be higher than the $\langle P_4 \rangle$ for 0% DG.

Lateral diffusion measurements

Using the excimer formation technique, the lateral diffusion constant D_L of the PE/DG mixtures was estimated by measuring the monomer lifetime of py-PC incorporated in the lipids (see Eq. 14). A diffusion length of l of 8 Å was used in the calculation (see Eq. 15 and 16). Fig. 5 showed the py-PC monomer lifetime and the calculated lateral diffusion constant as a function of DG%. An abrupt decline in the monomer lifetime was seen at ~6–8% DG. This corresponded to an increase in the lateral diffusion constant by ~50%. Based on the relationship between the hopping and lateral diffusion constants ($D_H = D_L/R^2$; R = radius of the lipid tubes), the values of R were computed and presented in Table 3. For 18% DG, R varied between 12–13 Å depending on the models. In comparison, for 0% DG, R varied between 127 Å to infinity. The latter was due to the confinement of setting D_H to zero for the WOBHOP model.

DISCUSSION

Both the wobbling and lateral diffusion may influence the rate of fluorescence anisotropy decay of fluorophores in lipid mixtures exhibiting H_{II} phase. In the H_{II} phase, the

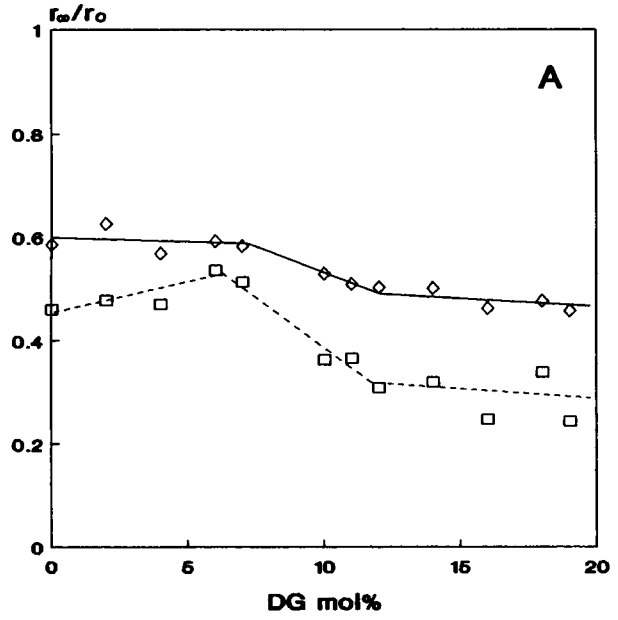

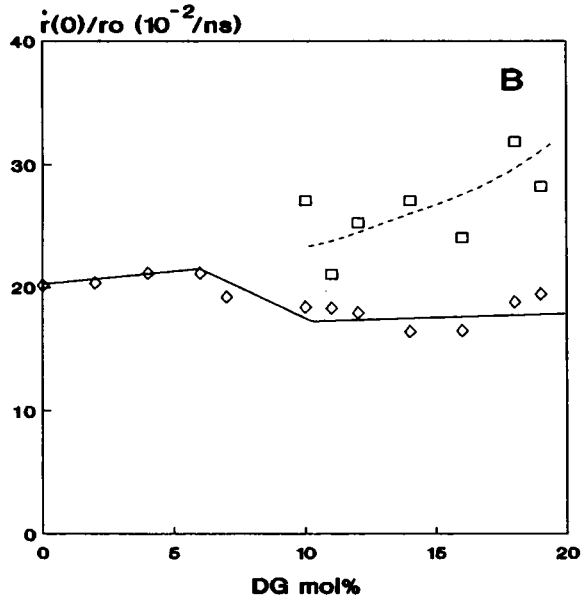

FIGURE 2 (*A*) Normalized residual anisotropy r_∞/r_0 of DPH-PC in PE/DG lipid mixtures as a function of DG content from one-exponential (◇) and two-exponential (□) fits. (*B*) Normalized initial slope of anisotropy decay $\dot{r}(0)/r_0$ of DPH-PC in PE/DG lipid mixtures as a function of DG content from one-exponential (◇) and two-exponential (□) fits.

lipids are arranged in a two-dimensional hexagonal lattice. Moreover, the physical dimension of the hexagonally packed lipid tubes, e.g., the radius of the tubes, is similar to that of a lipid (Tate and Gruner, 1989). Therefore, the magnitude of the rotational diffusion (hopping) constant D_H of the excited fluorophores around the highly curved

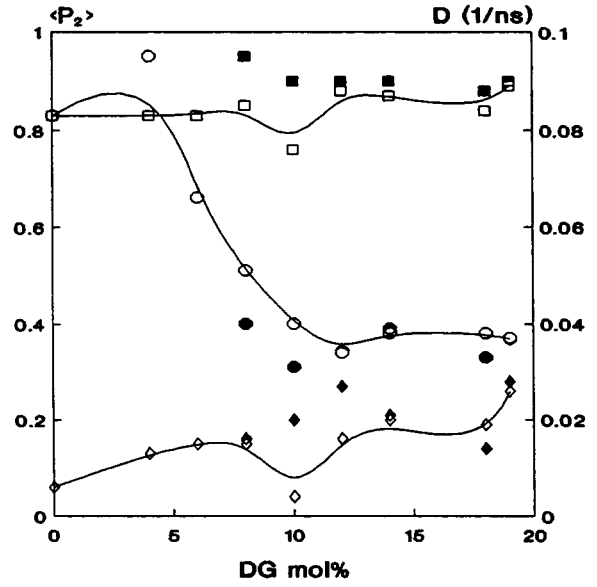

FIGURE 3 The second rank order parameter $\langle P_2 \rangle$ (□), wobbling diffusion constant D_W (○), and hopping diffusion constant D_H (◇) of DPH-PC in PE/DG lipid mixtures as a function of DG content from the WOBHOP model. The corresponding values obtained from the reduced WOBHOP model are also shown with filled symbols.

lipid tubes should be comparable with that of the wobbling diffusion constant D_W. The axes of rotation for D_H and D_W are along the long symmetry axis of the lipid tubes and perpendicular to the local symmetry axis of the lipids, respectively.

In this study, both empirical and molecular models were employed to analyze our fluorescence anisotropy data. Note that an empirical model provides only semiquantitative information about the orientational and dynamic nature of the fluorophore. This is accomplished by calculating the normalized long time residual (r_∞/r_0) and initial slope $(\dot{r}(0)/r_0)$ of $r(t)$. In contrast, a molecular model allows one to directly derive the physical parameters, e.g., orientational parameters and diffusion constants, from $r(t)$. For the WOBHOP model, the motional dynamics of the fluorophores are described by a steady state orientational factor $\langle P_2 \rangle$ and two diffusion constants, D_W and D_H. To get more detailed information about the orientational distribution of the fluorophore, a more sophisticated decay function (P2P4HOP model) was employed. This P2P4HOP model allows one to determine not only $\langle P_2 \rangle$, D_W, D_H, and r_0, but also $\langle P_4 \rangle$, the fourth-rank order parameter of the fluorophore.

The occurrence of a lipid phase transition is judged by the appearance of abrupt changes in the values of r_∞/r_0 and $\dot{r}(0)/r_0$. Generally speaking, these two parameters are related to the averaged orientational order and rotational rate of the fluorophores in lipid mixtures (Van

TABLE 3 **Fitted parameters for different anisotropy decay functions**

Sample	r_0	D_W	D_H	$\langle P_2 \rangle$	$\langle P_4 \rangle$	x^2	R
WOBHOP MODEL							
		$10^7\ s^{-1}$	$10^7\ s^{-1}$				Å
0% DG	0.24	5.32	0*	0.75	—	1.38	∞
18% DG	0.24	2.93	2.56	0.91	—	0.71	12.2
P2P4HOP MODEL							
0% DG	0.24	8.6	0.02	0.75	0.4	1.12	127.1
	(0.228, 0.244)‡	(5.0, 10.0)‡	(0.00, 0.19)‡	(0.74, 0.79)‡	(0.1, 0.57)‡		(41, ∞)‡
18% DG	0.24	8.0	2.2	0.89	0.58	0.81	13.2
	(0.228, 0.244)‡	(5.0, 25.0)‡	(0.03, 5.0)‡	(0.83, 0.91)‡	(−0.37, 0.66)‡		(8.6, 35.7)‡

*A fixed value, $D_H = 0$, was used for 0% DG in the case of the WOBHOP model.
‡Values between parentheses represent the 67% confidence interval (lower bound, upper bound) for the recovered value reported directly above this interval. $R = (D_H/D_L)^{1/2}$, where D_L (lateral diffusion constant) was obtained from measurements of the excimer formation rate (see Materials and Methods, and Fig. 5).

Der Meer et al., 1984; Cheng, 1989*a–c*). Abrupt changes in those averaged steady state and dynamic parameters are attributed to the alterations in the local order packing and packing symmetry of the lipids, and also to the modes of interactions of the fatty acyl chains with the fluorophores at the L_α-H_{II} transition (Cheng, 1989*a–c*). From the one-exponential fit, sudden declines in both r_∞/r_0 and $r(0)/r_0$ are found at ~6–8% DG. Interestingly, a previous time-resolved anisotropy decay study on dioleoyl PE (Cheng, 1989*a*) reveals that the declines in these parameters are correlated with the known L_α-H_{II} phase transition of the lipids. Therefore, it is concluded that an L_α-H_{II} phase transition occurs at ~6–8% DG in our present PE/DG system. By using the two-exponential model, a better chisquare and two well-separated rotational correlation times can be obtained for DG contents ranging from 10 to 18% (in the H_{II} phase). But for lower DG contents, large uncertainties in the short correlation time components and no improvement on the chisquares were observed. We concluded that the fluorophores exhibit a more complicated anisotropy decay behavior in the H_{II} phase than in the L_α phase.

The effects of DG on the polymorphic phase behavior of phospholipids have been studied extensively by x-ray diffraction, ^{31}P NMR, and differential scanning calorimetry (Das and Rand, 1986; Epand et al., 1988). Using an identical PE/DG lipid system, three phases are discerned at 23°C. They are L_α (0–6% DG), L_α/H_{II} (6–8% DG) and H_{II} (>10% DG) (Rand et al., 1990). The abrupt changes in the fitted parameters at ~6–8% DG correspond rather well with the above prediction of a L_α-H_{II} phase transition.

Between 6 and 8% DG, the lipids are in the coexisting L_α/H_{II} phase. No anomalous decline in the limiting anisotropy is found in this coexisting phase range. According to our theory (see the preceding paper), the limiting anisotropy in the L_α/H_{II} coexisting phase region should decrease monotonously instead of showing a singularity point with increasing H_{II} phase component. The latter was proposed by Johansson and Lindblom (1983). Interestingly, the isotropic/inverted cubic phase was recently hypothesized for a similar PE/DG lipid mixtures (Siegel et al., 1989). Yet our fluorescence data cannot distinguish whether the intermediate phase consists exclusively of coexisting L_α/H_{II}, isotropic/inverted, or both phases. However, the dynamics of the lipids in the intermediate phase appear to represent an average of that in the L_α and H_{II} phases within the fluorescence time scale.

The WOBHOP model reveals an increase in the local order parameter $\langle P_2 \rangle$ but a decrease in the wobbling diffusion constant D_W as the lipids change from the L_α to H_{II} phase. This higher local order parameter and slower wobbling diffusion of fluorophores in the H_{II} phase may be induced by the enhanced packing constraint of the lipid molecules at the lipid/water interface. Similar results were also found in our previous study (Cheng, 1989*a*) as well as in a recent angular resolved fluorescence study (van Langen et al., 1989). Diolein in this study has a small head group and two bulky oleic fatty acyl chains hydrocarbon chains as compared to PE. This observed increase in the order parameter supports the notion that DG perturbs the intrinsic curvature of PE lipid bilayers by furnishing a larger hydrocarbon volume per average lipid molecule in the lipid mixture. A significant increase in the hopping diffusion constant D_H from the L_α to H_{II} phase is evident from the results obtained by using both the WOBHOP and P2P4HOP models. Theoretically, the lateral diffusion of fluorophores in the planar L_α phase should not contribute to fluorescence anisotropy decay of the fluorophore. The analysis using the P2P4HOP model gives a value of D_H statistically equivalent to zero. This result agrees well with the theoretical prediction.

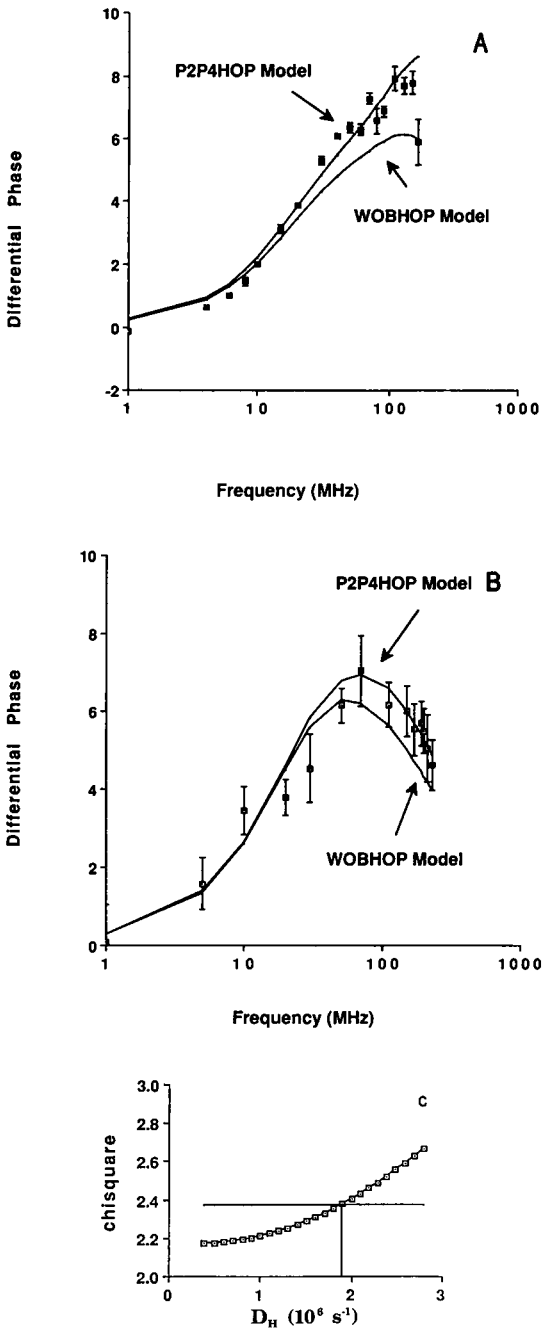

FIGURE 4 (*A*) Fitted curves for the differential polarized phase angle versus modulation frequency of DPH-PC in 0% DG using WOBHOP and P2P4HOP models. (*B*) Fitted curves for the differential polarized phase angle versus modulation frequency of DPH-PC in 18% DG using WOBHOP and P2P4HOP models. (*C*) Rigorous confidence intervals (67%) for hopping diffusion constant D_H at 0% DG using the P2P4HOP model.

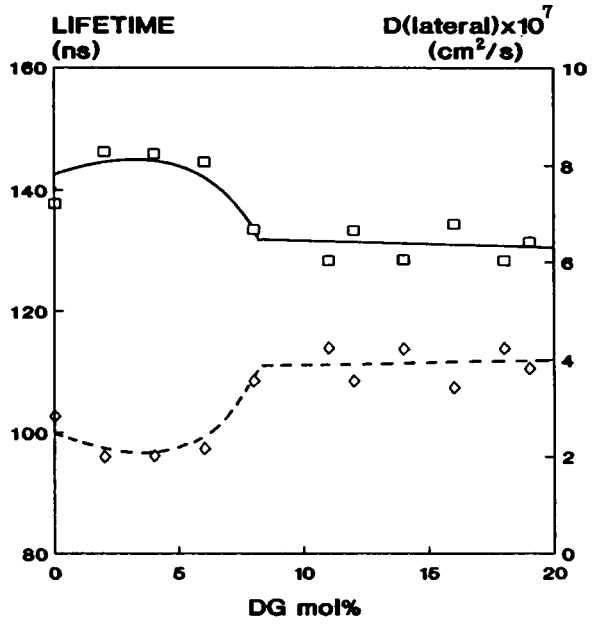

FIGURE 5 Fluorescent lifetime of monomer emission (□) and calculated lateral diffusion constant (◊) of py-PC in DG/TPE lipid mixtures as a function of DG content.

The two-exponential model yields a fit comparable to the ones for the more elaborate WOBHOP and P2P4HOP models for lipids in the H_{II} phase (10–18% DG). Yet the two rotational correlation times are well-resolved by the two-exponential model. Note that the correlation time attributed to the hopping motion is longer than that of the wobbling time, i.e., $\tau_H/\tau_W \approx 10$. Under this consideration, it is therefore not surprising that the anisotropy decay of fluorophores can well be described by a simple two-exponential decay model (reduced WOBHOP model).

The physical origin of the extra hopping motion of fluorophores in the H_{II} phase is the lateral diffusion motion of the fluorophores over the highly curved lipid tubes. By comparing the hopping diffusion constant obtained from the anisotropy measurements and the lateral diffusion constant obtained from the excimer formation measurements, the radius of curvature of the lipid tubes has been determined. The radius falls into a range of 10–15 Å in our PE/DG lipid mixtures. These values are of the same order of magnitude as those obtained from x-ray diffraction (Tate and Gruner, 1989).

It should be noted, however, that the observation that the WOBHOP and P2P4HOP models fit the data may not prove that the two models are necessarily correct. Of course it may be argued that the agreement between experiment and theory is purely coincidental. Nevertheless, we feel that the assumptions on which our models are

based are reasonable and that the fact that the values for the radius of the hexagonal tube we find is of the right order of magnitude provide strong support for the validity of our proposed molecular models.

In summary, new molecular models (WOBHOP and P2P4HOP) for time-resolved fluorescence anisotropy decay have provided more detailed information and insights in understanding the orientational order and rotational dynamics of lipid molecules in the H_{II} phase. The reasonable prediction of the size of the lipid tubes from this time-resolved fluorescence study further validates our theoretical models. The use of time-resolved fluorescence technique to measure the size of lipid tubes in the H_{II} phase represents an innovative approach to obtain structural information of fully hydrated lipid/water systems.

The enlightening discussion with Dr. Sol. M. Gruner of Princeton University, regarding the size of the lipid hexagonal tubes, is gratefully acknowledged.

This work was supported by grants from the National Institutes of Health (Ca 47610) and the Robert A. Welch Foundation (D-1158) given to Dr. Cheng. Dr. Chen is a recipient of the Robert A. Welch Research Foundation scholarship. Dr. Van Der Meer acknowledges support by the National Science Foundation and the Kentucky EPSCOR Program (RII-8610671). Dr. Beechem acknowledges the support of the Lucille P. Markey Foundation.

Received for publication 25 May 1990 and in final form 2 August 1990.

REFERENCES

Ameloot, M., H. Hendricks, W. Herreman, F. Van Canwelaert, and B. W. Van Der Meer. 1984. Effect of orientational order on the decay of the fluorescence anisotropy in membrane suspensions. Experimental verification on unilamellar vesicles and lipid/α-lactalbumin complexes. *Biophys. J.* 46:247–256.

Beechem, J. M., and E. Haas. 1989. Simultaneous determination of intramolecular distance distributions and conformational dynamics by global analysis of energy transfer measurements. *Biophys. J.* 55:1225–1236.

Cheng, K. H. 1989*a*. Fluorescence depolarization study of lamellar liquid crystalline to inverted cylindrical micellar phase transition of phosphatidylethanolamine. *Biophys. J.* 55:1025–1031.

Cheng, K. H. 1989*b*. Fluorescence depolarization study on non-bilayer phases of phosphatidylethanolamine and phosphatidylcholine lipid mixtures. *Chem. Phys. Lipids.* 51:137–145.

Cheng, K. H. 1989*c*. Time-resolved fluorescence depolarization study of lamellar to inverted cylindrical micellar phase. Fluorescence Detection III. E. Roland Menzel, editor. *Proc. SPIE.* 1054:160–167.

Cheng, K. H., and S. W. Hui. 1986*a*. Correlation between bilayer destabilization and activity enhancement by diacylglycerols in reconstituted Ca-ATPase vesicles. *Arch. Biochem. Biophys.* 244:382–386.

Cheng, K. H., J. R. Lepock, S. W. Hui, and P. L. Yeagle. 1986*b*. The role of cholesterol in the activity of reconstituted Ca-ATPase vesicles containing unsaturated phosphatidylethanolamine. *J. Biol. Chem.* 261:5081–5087.

Chong, P. L., and T. E. Thompson. 1985. Oxygen quenching of pyrene-lipid fluorescence in phosphatidylcholine vesicles. A probe for membrane organization. *Biophys. J.* 47:613–621.

Crowe, L. M., and J. H. Crowe. 1982. Effects of dehydration on membranes and membrane stabilization at low water activities. *In* Biological Membranes. D. Chapman, editor. Academic Press, London, 5:58–98.

Das, S., and R. P. Rand. 1986. Modification by diacylglycerol of the structure and interaction of various phospholipid bilayer membranes. *Biochemistry.* 25:2882–2889.

Ellens, H., D. P. Siegel, D. Alford, P. L. Yeagle, L. Boni, L. J. Lis, P. J. Quinn, and J. Bentz. 1989. Membrane fusion and invertd phases. *Biochemistry.* 28:3692–3703.

Expand, R. M., R. F. Epand, and C. R. Lancaster. 1988. Modulation of the bilayer to hexagonal phase transition of phosphatidylethanolamines by acylglycerols. *Biochim. Biophys. Acta.* 945:161–166.

Gallas, H.-J., W. Hartmann, U. Theilen, and E. Sackmann. 1979. On two-dimensional passive random walk in lipid bilayers and fluid pathways in biomembranes. *J. Membr. Biol.* 48:215–236.

Gratton, E., D. M. Jameson, and R. D. Hall. 1984. Multifrequency phase and modulation fluorometry. *Annu. Rev. Biophys. Bioeng.* 13:105–124.

Johansson, L. B.-A., and G. Lindblom. 1983. Application of time resolved luminescence in the study of lipid aggregate symmetry. I. Theoretical discussion. *J. Chem. Phys.* 78:1519–1522.

Kirk, G. L., and S. M. Gruner. 1985. Lyotropic effects of alkanes and headgroup composition of the L_α-H_{II} lipid liquid crystal phase transition: hydrocarbon packing versus intrinsic curvature. *J. Physique.* 46:761–769.

Lakowicz, J. R. 1983. Principle of fluorescence spectroscopy. Plenum Press, New York. 127.

Lakowicz, J. R., and B. P. Maliwal. 1985. Construction and performance of a variable frequency phase-modulation fluorometer. *Biophys. Chem.* 21:61–78.

Luzzati, V., and F. Husson. 1962. The structure of the liquid-crystalline phases of lipid-water systems. *J. Cell Biol.* 12:207–219.

Parente, R. A., and B. R. Lentz. 1985. Advantages and limitations of 1-palmitoyl-2-[[2-[4-(6-phenyl-trans-1,3,5-hexatrienyl)phenyl]ethyl]-3-*sn*-phosphatidylcholine as a fluorescent probe. *Biochemistry.* 24: 6178–6185.

Rand, R. P., N. L. Fuller, S. M. Gruner, and V. A. Parsegian. 1990. Membrane curvature, lipid segregation, and structural transitions for phospholipids under dual-solvent stress. *Biochemistry.* 29:76–87.

Siegel, D. P., J. Banschbach, D. Alford, J. Ellens, L. J. Lis, P. J Quinn, P. L. Yeagle, and J. Bentz. 1989. Physiological levels of Diacylglycerols in phospholipid membranes induce membrane fusion and stabilize inverted phases. *Biochemistry.* 28:3703–3709.

Spencer, R. D., and G. Weber. 1970. Influence of Brownian rotations and energy transfer upon the measurements of fluorescence lifetime. *J. Chem. Phys.* 52:1654–1663.

Straume, M., and B. J. Litman. 1987. Equilibrium and dynamic structure of large, unilamellar, unsaturated acyl chain phosphatidylcholine vesicles. *Biochemistry.* 26:5113–5120.

Szabo, A. 1980. Theory of polarized fluorescent emission in uniaxial liquid crystals. *J. Chem. Phys.* 72:4620–4626.

Tate, M. W., and S. M. Gruner. 1989. Temperature dependence of the structural dimensions of the inverted hexagonal (H_{II}) phase of phosphatidylethanolamine-containing membranes. *Biochemistry.* 28: 4245–4253.

Van Der Meer, W., H. Pottel, W. Herreman, M. Ameloot, H. Hendrickx, and H. Schröder. 1984. Effect of orientational order on the decay of the fluorescence anisotropy in membrane suspensions. *Biophys. J.* 46:515–523.

van Langen, H., D. A. Schrama, G. van Ginkel, G. Ranke, and Y. K. Levin. 1989. Order and dynamics in the lamellar L_α and in the hexagonal H_{II} phase. *Biophys. J.* 55:937–947.

Zannoni, C., A. Arcioni, and P. Cavatarta. 1983. Fluorescence depolarization in liquid crystals and membrane bilayers. *Chem. Phys. Lipids.* 32:179.